Dalton Transactions

Cite this: *Dalton Trans.*, 2011, **40**, 8340

www.rsc.org/dalton

PAPER

3,4,3-LI(1,2-HOPO): *In vitro* formation of highly stable lanthanide complexes translates into efficacious *in vivo* europium decorporation†

Manuel Sturzbecher-Hoehne,[a] Clara Ng Pak Leung,[a] Anthony D'Aléo,[a] Birgitta Kullgren,[a] Anne-Laure Prigent,[a] David K. Shuh,[a] Kenneth N. Raymond[a,b] and Rebecca J. Abergel*[a]

Received 4th May 2011, Accepted 6th June 2011
DOI: 10.1039/c1dt10840a

The spermine-based hydroxypyridonate octadentate chelator 3,4,3-LI(1,2-HOPO) was investigated for its ability to act as an antenna that sensitizes the emission of Sm^{III}, Eu^{III}, and Tb^{III} in the Visible range (Φ_{tot} = 0.2–7%) and the emission of Pr^{III}, Nd^{III}, Sm^{III}, and Yb^{III} in the Near Infra-Red range, with decay times varying from 1.78 µs to 805 µs at room temperature. The particular luminescence spectroscopic properties of these lanthanide complexes formed with 3,4,3-LI(1,2-HOPO) were used to characterize their respective solution thermodynamic stabilities as well as those of the corresponding La^{III}, Gd^{III}, Dy^{III}, Ho^{III}, Er^{III}, Tm^{III}, and Lu^{III} complexes. The remarkably high affinity of 3,4,3-LI(1,2-HOPO) for lanthanide metal ions and the resulting high complex stabilities (pM values ranging from 17.2 for La^{III} to 23.1 for Yb^{III}) constitute a necessary but not sufficient criterion to consider this octadentate ligand an optimal candidate for *in vivo* metal decorporation. The *in vivo* lanthanide complex stability and decorporation capacity of the ligand were assessed, using the radioactive isotope ^{152}Eu as a tracer in a rodent model, which provided a direct comparison with the *in vitro* thermodynamic results and demonstrated the great potential of 3,4,3-LI(1,2-HOPO) as a therapeutic metal chelating agent.

Introduction

Siderophore-inspired multidentate hydroxypyridonate ligands can be used in a variety of applications such as magnetic resonance imaging (MRI) contrast enhancement, lanthanide luminescence sensitization, and iron and actinide chelation.[1–5] The octadentate ligand 3,4,3-LI(1,2-HOPO) (Fig. 1), composed of four 1-hydroxy-pyridin-2-one (1,2-HOPO) units linked to a spermine scaffold through amide linkages, is currently considered the most efficient experimental decorporation agent for actinides.[1,6,7] Studies have shown that this ligand is orally active and is by far more efficacious than the commonly used diethylenetriamine-pentaacetic acid (DTPA, Fig. 1) at promoting the *in vivo* decorporation of actinide metal ions, such as U^{VI}, Np^{V}, Pu^{IV}, and Am^{III}.[6–8] In addition, 3,4,3-LI(1,2-HOPO) is known to act as an antenna that sensitizes the luminescence of Eu^{III}, a feature that was used recently to determine the solution thermodynamic stability of the corresponding $[Eu^{III}(3,4,3\text{-LI}(1,2\text{-HOPO}))]^{-}$ complex.[9] In the work presented here, the photophysical properties of the complexes of 3,4,3-LI(1,2-HOPO) formed with metal ions from the whole lanthanide series were probed and characteristic emission sensitization was observed in both the Visible and Near Infra-Red ranges, depending on the complexed metal ion. The use of the antenna effect as a spectroscopic tool was extended to spectrofluorimetric competition titrations, to determine the formation constants of these lanthanide complexes. While such thermodynamic parameters are essential to characterize 3,4,3-LI(1,2-HOPO) as a chelating agent and compare its affinity to different metal ions, they are only indicative of the potential *in vivo* decorporation efficacy of the ligand. The *in vivo* Eu^{III} complex stability and Eu^{III} decorporation capacity of 3,4,3-LI(1,2-HOPO) were therefore also assessed in mice, using the radioactive isotope ^{152}Eu as a contaminant, which provides a direct comparison with the *in vitro* thermodynamic results.

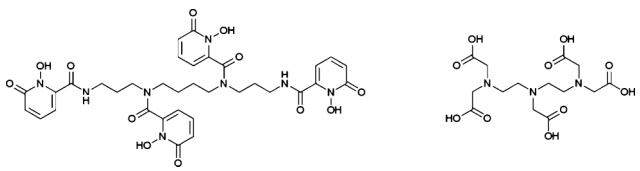

Fig. 1 Structures of the experimental octadentate ligand 3,4,3-LI(1,2,-HOPO) (left) and the approved decorporation agent DTPA (right).

[a]*Chemical Sciences Division, Lawrence Berkeley National Laboratory, Berkeley, CA, 94720, USA. E-mail: rjabergel@lbl.gov; Fax: +1 510 486 5596; Tel: +1 510 486 5249*
[b]*Department of Chemistry, University of California, Berkeley, CA, 94720-1460, USA*

† Electronic supplementary information (ESI) available: Lanthanide complexes electronic absorption spectra and full radioanalysis data sets for *in vivo* experiments. See DOI: 10.1039/c1dt10840a

Experimental

General considerations

All chemicals were obtained from commercial suppliers and used as received. The Ln^{III} salts utilized were of the highest purity available (>99.9%). The ligand 3,4,3-LI(1,2-HOPO) was synthesized by Synthetech, Inc. (Albany, OR, USA), following previously reported procedures, and used as received. A Millipore Milli-Q Advantage A10 Water System Production Unit was used to purify deionized water.

Photophysics

UV-Visible absorption spectra were recorded either on a Varian Cary 300 double beam absorption spectrometer or Ocean Optics USB 4000, using quartz cells of 1.00 cm path length. Emission spectra were acquired on a HORIBA Jobin Yvon IBH FluoroLog-3 spectrofluorimeter, equipped with 3 slit double grating excitation and emission monochromators (2.1 nm mm^{-1} dispersion, 1200 grooves mm^{-1}). Spectra were reference corrected for both the excitation light source variation (lamp and grating) and the emission spectral response (detector and grating). Luminescence lifetimes were determined on a HORIBA Jobin Yvon IBH FluoroLog-3 spectrofluorimeter, adapted for time-correlated single photon counting (TCSPC) and multichannel scaling (MCS) measurements. A sub-microsecond Xenon flashlamp (Jobin Yvon, 5000XeF) was used as the lightsource, with an input pulse energy (100 nF discharge capacitance) of *ca.* 50 mJ, yielding an optical pulse duration of less than 300 ns at FWHM. Spectral selection was achieved by passage through a double grating excitation monochromator (2.1 nm mm^{-1} dispersion, 1200 grooves mm^{-1}). Emission was monitored perpendicular to the excitation pulse, again with spectral selection achieved by passage through a double grating excitation monochromator (2.1 nm mm^{-1} dispersion, 1200 grooves $/mm^{-1}$). A thermoelectrically cooled single photon detection module (HORIBA Jobin Yvon IBH, TBX-04-D) incorporating fast rise time PMT, wide bandwidth preamplifier and picosecond constant fraction discriminator was used as the detector. Signals were acquired using an IBH DataStation Hub photon counting module and data analysis was performed using the commercially available DAS 6 decay analysis software package from HORIBA Jobin Yvon IBH. Goodness of fit was assessed by minimizing the reduced chi squared function, χ^2, and a visual inspection of the weighted residuals. Each trace contained at least 5,000 points, and the estimated error on the reported lifetime values is ±10%. Quantum yields and kinetic parameters were determined as previously described.[9]

Mass spectrometry analysis

Mass spectra were obtained on an Agilent Technologies 6120 Quadrupole MS equipped with an electrospray ionization source. For direct injection, a syringe pump (KD Scientific) delivered the samples to the mass spectrometer with a constant flow rate of 83 µL min^{-1}. The voltage applied to the capillary was 3.2 kV in the negative detection mode. A nitrogen gas flow rate of 12 L min^{-1} was used to assist the nebulization process. The cone voltage was set in negative 50 V and the ion source temperature was 150 °C. Mass spectra were recorded over a 50–1100 m/z range. The pH of each injected solution was measured with a conventional pH meter at 25 °C (713 pH meter, Metrohm Brinkmann) that was equipped with a glass electrode (Micro Combi Electrode, Metrohm) filled with KCl and calibrated with pH standards. All samples were prepared in purified deionized water and special care was taken to adjust the pH to 7.4 with KOH (other bases and buffers may yield to additional peaks in the mass spectra).

Solution thermodynamics: General considerations

A Micro Combi Electrode (Metrohm) glass electrode (response to $[H^+]$ was calibrated before each titration)[10] was used with a Metrohm Titrando 907 (Metrohm) to measure the pH of the experimental solutions. The Metrohm autoburet adds incremental volumes of acid or base standard solutions to the titration cell. The titration instruments were fully automated and controlled using the Tiamo software from Metrohm. Titrations were performed in 0.1 M KCl supporting electrolyte under positive Ar gas pressure. The temperature of the experimental solutions was maintained at 25 °C by an external circulating water bath. Luminescence spectra for direct spectrofluorimetric titrations were recorded on an Ocean Optics USB 4000 spectrophotometer (slit 50 mm, grating 600 grooves mm^{-1}, blaze 400 nm) equipped with a PX-2 pulsed xenon or HPX-2 high-powered xenon light source. Samples were pumped trough a loop in an asymmetric fluorescence cell (2 × 10 mm, 40 µl) with a peristaltic pump after adding the increment of reagent. All titrant solutions were prepared using distilled water that was further purified by passing through a Millipore Milli-Q reverse osmosis cartridge system. Titrants were degassed by boiling for 1 h while being purged under Ar. Carbonate-free 0.1 M KOH was prepared from Baker Dilut-It concentrate and was standardized by titrating against 0.1 M HCl. Solutions of 0.1 M HCl were similarly prepared and were standardized by titrating against TRIS. Stock solutions of 3,4,3-LI(1,2-HOPO) were obtained by dissolving in Milli-Q water. Stock solutions of lanthanide ions were obtained by dissolving solid $LnCl_3 \cdot nH_2O$ in standardized 0.1 M HCl.

Eu^{III} complex: Incremental spectrofluorimetric titrations

Solutions were assembled from stock solutions of ligand, a measured aliquot of the europium stock solution and the supporting electrolyte solution, with resulting ligand and europium concentrations of ~ 50 µM, and were incrementally perturbed by the addition of titrant, followed by a time delay for equilibration (180 s). Buffering of the solution was assured by the addition of acetic acid, HEPES and MES buffers (10 mM). An average of 120–150 data points were collected in each pair of complex titrations, each data point consisting of a pH measurement and luminescence spectra over the pH range 1.4 to 10.5. Nonlinear least-squares refinement of the complex formation constants was performed using the program pHab.[10–14]

Ln^{III} complexes: Spectrofluorimetric competition batch titrations

Varying volumes of a Ln^{III} stock solution were added to solutions of ligand (0.03 mM) and europium (0.03 mM) in 0.1 M KCl buffered at pH 7.4 with 0.1 M HEPES. All solutions were diluted to identical volumes to reach final concentrations of ligand and europium of 0.005 mM. The ranges of Eu^{III}:Ln^{III} used in each

Table 1 Photophysical and thermodynamic parameters for $[Ln^{III}(3,4,3\text{-LI}(1,2\text{-HOPO}))]^-$ at pH 7.4[a]

Ln	La[b]	Pr[c]	Nd[c]	Sm	Eu	Gd[d]	Tb	Dy[e]	Ho[e]	Er[e]	Tm[d]	Yb[c]	Lu[f]
n, [Xe] $4f^n$	0	2	3	5	6	7	8	9	10	11	12	13	14
Photophysical parameters													
λ_{max} (nm)	320	316	317	316	315	316	316	315	315	315	315	315	314
ε_{max} ($M^{-1}cm^{-1}$)	16,460	17,080	17,220	17,850	17,740	17,830	17,810	17,470	17,790	17,620	17,790	17,880	16,760
Φ_{tot}				0.002(1)	0.07(1)[g]		0.002(1)						
τ_{obs} (μs)			122	17.4	805[g]		10.0					1.78	
Thermodynamic parameters													
log K_{ML}	16.4(3)	18.2(4)	18.7(1)	19.7(3)	20.2(2)	20.5(1)	20.9(1)	21.2(1)	21.5(1)	21.7(1)	22.0(1)	22.2(1)	21.2(1)
pM‡	17.2(3)	19.0(4)	19.6(1)	20.6(3)	21.1(2)[g]	21.3(1)	21.8(1)	22.1(1)	22.4(1)	22.6(1)	22.9(1)	23.1(1)	22.0(1)
ΔpM[h]	–3.9	–2.1	–1.5	–0.5	0	0.2	0.7	1.0	1.3	1.5	1.8	2.0	0.9

[a] The figures in parentheses give the uncertainty determined from the standard deviation between three independent measurements, all values reported are for $I = 0.1$ M (KCl); [b] no f electron; [c] no reference in the NIR to calculate ϕ_{tot}; [d] no sensitization possible; [e] no sensitization observed; [f] full electron shell; [g] previously reported;[9] [h] $[Eu^{III}(3,4,3\text{-LI}(1,2\text{-HOPO}))]^-$ is used as a reference with a pM‡ value of 21.1.

competition titration were: 1 : 0 to 1 : 1000 for La^{III}, 1 : 0 to 1 : 100 for Pr^{III} and Nd^{III}, and 1 : 0 to 1 : 10 for $Ln^{III} = Sm^{III}$–Lu^{III}.

All samples were equilibrated in a thermostatic shaker at 25 °C until equilibrium was reached and measurements were stable (5 d). The emission spectrum of each solution was measured using a 1-cm quartz cell (λ_{exc} = 325 nm, λ_{em} = 570–720 nm). The data were then imported into the refinement program HypSpec[10–15] and analyzed by nonlinear least-squares refinement.

Solution thermodynamics: Data treatment

All equilibrium constants were defined as cumulative formation constants, β_{mlh} according to eqn (1), where the metal and ligand are designated as M and L, respectively.

$$mM + lL + hH \leftrightarrow [M_mL_lH_h]; \beta_{mlh} = \frac{[M_mL_lH_h]}{[M]^m[L]^l[H]^h} \quad (1)$$

All metal and ligand concentrations were held at estimated values determined from the volume of standardized stock solutions. The refinements of the overall formation constants β_{110} and β_{111} included in each case the four previously determined ligand protonation constants[9] and the metal hydrolysis products, for which equilibrium constants were fixed to the literature values[16] (Table 2 and ESI† Table S1); all ligand species formed with Eu^{III}, Sm^{III} or Tb^{III} were considered to have significant emission to be observed in the emission spectra. The pM(Ln^{III})‡ values were calculated using the modelling program Hyss.[17,18]

In vivo evaluation: General considerations

All procedures and protocols used in the presented *in vivo* studies were reviewed and approved by the Institutional Animal Care and Use Committee of the Lawrence Berkeley National Laboratory and were performed in AAALAC accredited facilities. The animals used were young adult female Swiss-Webster mice (87 ± 9 days old, 32 ± 2 g). After injection of a ^{152}Eu tracer, mice were weighed, identified, and housed in groups of five in plastic stock cages lined with a 0.5 cm layer of highly absorbent low-ash pelleted cellulose bedding (Alpha-dry) for separation of urine and feces. All mice were given water and food *ab libitum* and were euthanized at 24 h after the tracer injection. All experiments using ^{152}Eu tracers were managed as metabolic balance studies, in which blood, all tissues, and excreta were analyzed for ^{152}Eu by liquid scintillation counting on a Perkin Elmer Packard Tri-Carb model B4430. The methods of sample collection, preparation, radioactivity measurements, and data reduction have been published previously.[19,7,20,21] Those methods provide quantitative measurements of the radioactivity in the biological samples and material recoveries are about 95% of the amount injected.

‡ pM is the –log [free M] for the specific set of conditions [Metal] = 10^{-6} M, [Ligand] = 10^{-5} M, pH 7.4.

Table 2 Protonation and Eu^{III} complex formation constants for 3,4,3-LI(1,2-HOPO)

Species	*m*, *l*, *h*	log β_{mlh}
LH	0, 1, 1	6.64(1)[a]
LH_2	0, 1, 2	12.32(1)[a]
LH_3	0, 1, 3	17.33(1)[a]
LH_4	0, 1, 4	21.20(1)[a]
EuL	1, 1, 0	20.2(2)[b]
EuLH	1, 1, 1	21.4(2)[b]
pEu^{III}		21.1(2)[b]

[a] Previously determined and reported.[9] [b] Values experimentally determined in this work, following a previously reported method[9] with modified additional titrant increments for more accurate measurements.

Decorporation efficacy assay

Ligand solutions were prepared such that the selected dosage (30 μmol kg^{-1}) was contained in 0.5 mL of 0.14 M NaCl, the pH being adjusted to 7.4–8.4 with 1 N NaOH. Under isoflurane anesthesia, groups of five normally fed mice were injected in a lateral tail vein with 0.2 mL of the tracer solution containing ^{152}Eu (1.7 kBq, 0.024 ng) in 0.008 M sodium citrate and 0.14 M NaCl, pH 4. Ligands were administered by intraperitoneal injection at 1 h after the tracer injection. Isotonic saline was administered to control animals.

In vivo complex stability Assay

The ^{152}Eu complexes of DTPA and 3,4,3-LI(1,2-HOPO) were prepared *in situ* at molar ratio ligand:^{152}Eu > 20 by mixing and incubating the appropriate quantities of $^{152}EuCl_3$ and ligand in

0.14 M NaCl to reach a ^{152}Eu concentration of 0.12 μg L^{-1}. Under isoflurane anesthesia, groups of five normally fed mice were injected intraperitoneally with 0.2 mL of a complex solution (1.7 kBq per mouse).

Results and discussion

Photophysical characterization

The photophysical parameters for the lanthanide complexes $[Ln^{III}(3,4,3\text{-LI}(1,2\text{-HOPO}))]^-$ (Ln from La^{III} to Lu^{III}, excluding Pm^{III} and Ce^{III}; Pm^{III} was excluded due to its radioactivity while Ce^{III} was excluded because of its reduction/oxidation properties) were measured in buffered aqueous solutions at pH 7.4 and are summarized in Table 1. The electronic absorption spectra show a shift towards the higher energies along the lanthanide series, with an absorption maximum due to the ligand $\pi \rightarrow \pi^*$ transitions that ranges from λ_{max} = 320 nm for La to λ_{max} = 314 for Lu (See ESI† Fig. S1). Luminescence spectra were recorded for all complexes with the same excitation wavelength λ_{exc} = 325 nm. Based on the ligand triplet excited state determined previously,[9] 3,4,3-LI(1,2-HOPO) was expected to sensitize the luminescence of most lanthanides other than Eu^{III}, except La^{III} (no f-electron), Lu^{III} (full electron shell), Gd^{III} and Tm^{III} (emitting f-orbitals higher in energy).[22] Sensitized emission was observed in the visible range for the Sm^{III} and Tb^{III} complexes and in the Near Infra-Red range for the Pr^{III}, Nd^{III}, Sm^{III}, and Yb^{III} complexes (Fig. 2), while no luminescence was observed for the Dy^{III}, Ho^{III} and Er^{III} complexes. Time-resolved analysis of the luminescence of the emitting complexes revealed monoexponential decays with decay times varying from 1.78 μs to 805 μs at room temperature. The luminescence quantum yields of the two complexes emitting in the visible, $[Sm^{III}(3,4,3\text{-LI}(1,2\text{-HOPO}))]^-$ and $[Tb^{III}(3,4,3\text{-LI}(1,2\text{-HOPO}))]^-$, were both determined with the optically dilute method (with optical density < 0.1); the resulting values (Φ_{tot} = 0.2% for both) were significantly lower than that of the Eu^{III} complex (7.0%),[9] which can be attributed to the closeness between the ligand triplet excited state and the emitting excited states of Sm^{III} and Tb^{III}, and the corresponding energy transfer/back-transfer processes.

Solution thermodynamics

A direct spectrofluorimetric titration method had been described previously to determine the Eu^{III} complex formation constants for 3,4,3-LI(1,2-HOPO).[9] The spectral measurements relied on the sensitization of the Eu luminescence by the excited ligand: the emission intensity of a solution containing equimolar amounts of Eu^{III} and ligand increased upon pH increase and resulting complex formation (Fig. 3). The Eu^{III} complex formation constants were re-determined in this work, following this direct spectrofluorimetric method,[9] with modified additional titrant increments that allowed more accurate measurements (Table 2).

As only two lanthanides other than Eu^{III} are sensitized by 3,4,3-LI(1,2-HOPO) to emit luminescence in the visible region (albeit with very low quantum yields), a systematic determination of the stability constants of each complex was not possible through the direct titration method. However, proton-independent stability constants ($K_{ML} = \beta_{110}$) and corresponding conditional stability constants (calculated and reported as pM values)‡ for the lanthanide series could be determined indirectly through metal competition titrations (Table 1), using Eu^{III} as a reference because of its central position in the series and the remarkable luminescence properties of the corresponding 3,4,3-LI(1,2-HOPO) complex. In these competition titrations, solutions containing an equimolar ratio of Eu^{III} and 3,4,3-LI(1,2-HOPO) ($[Eu^{III}]$ = [3,4,3-LI(1,2-HOPO)] = 5 μM, [KCl] = 0.1 M, [HEPES] = 0.1 M, pH 7.4, 25.0 °C) were divided into separate aliquots and the studied lanthanide was added to reach concentrations varying from 0 to 5 mM. The solutions were allowed to reach equilibrium (when no luminescence change was observed) and the emission spectra recorded (λ_{exc} = 325 nm). The intensity of the $[Eu^{III}(3,4,3\text{-LI}(1,2\text{-HOPO}))]^-$ emission decreases upon addition of the competing lanthanide (Fig. 4), dependent on its affinity for the ligand, and corresponding to the formation of the new complex. The data consisting of sets of emission spectra (λ_{em} = 570–720 nm) with varying concentrations of competing lanthanide ion were imported into the refinement program HypSpec[15] and analyzed by nonlinear least-squares refinements. The equilibration of 3,4,3-LI(1,2-HOPO) between Eu^{III} and the competing metal was calculated by including the proton association and Eu^{III} complex formation constants of

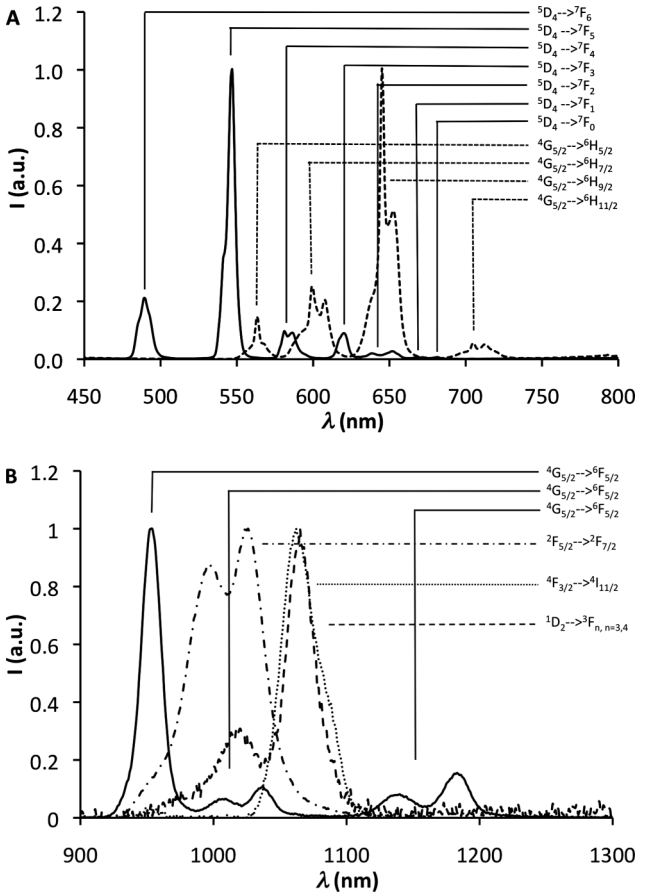

Fig. 2 Luminescence spectra in buffered aqueous solutions, pH = 7.4, 0.1 M HEPES, λ_{exc} = 325 nm of: **A)** $[Sm^{III}(3,4,3\text{-LI}(1,2\text{-HOPO}))]^-$ (solid) and $[Tb^{III}(3,4,3\text{-LI}(1,2\text{-HOPO}))]^-$ (dash); **B)** $[Pr^{III}(3,4,3\text{-LI}(1,2\text{-HOPO}))]^-$ (dash), $[Nd^{III}(3,4,3\text{-LI}(1,2\text{-HOPO}))]^-$ (dot), $[Sm^{III}(3,4,3\text{-LI}(1,2\text{-HOPO}))]^-$ (solid), $[Yb^{III}(3,4,3\text{-LI}(1,2\text{-HOPO}))]^-$ (dash dot). Spectra are normalized to the highest emission peak and emission peaks are labelled with the specific corresponding transition.

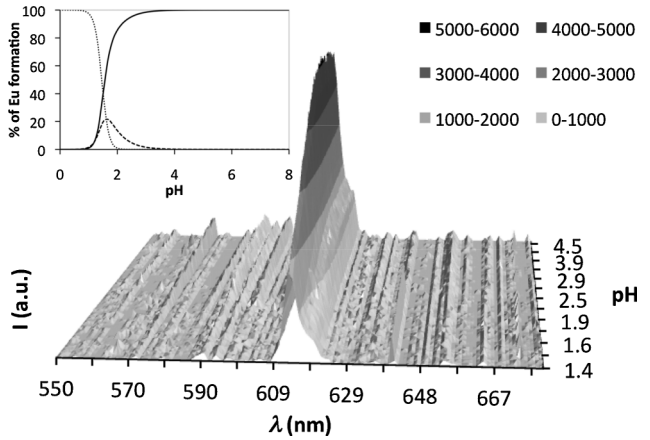

Fig. 3 Re-determination of the stability constants of the $[Eu^{III}(3,4,3\text{-LI}(1,2\text{-HOPO}))]^-$ complex through direct spectrofluorimetric titration ($[Eu^{III}]$ = [3,4,3-LI(1,2-HOPO)] = 0.05 mM, 0.1 M KCl, 10 mM MES, 10 mM acetic acid, 25 °C, λ_{exc} = 325 nm, pH 1.3 to 10). Emission spectra shown for the pH range of 1.4–4.5; the luminescence signal increases with the pH, which allows the determination of the stability constants.[9] **Inset.** Eu species distribution in the titration conditions: dotted line = free Eu; dashed line = EuLH; solid line = EuL^-.

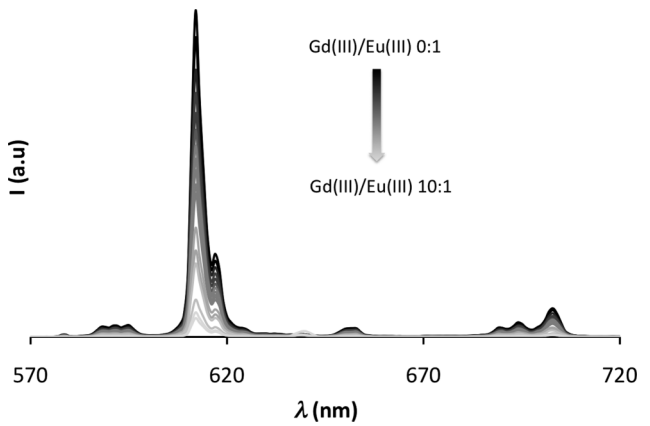

Fig. 4 Spectrofluorimetric competition titration of $[Eu^{III}(3,4,3\text{-LI}(1,2\text{-HOPO}))]^-$ against Gd(III). $[Eu^{III}]$ = [3,4,3-LI(1,2-HOPO)] = 5 μM, $[Gd^{III}]$ = 0–0.05 mM, 0.1 M KCl, 0.1 M HEPES, pH = 7.4, 25.0 °C, λ_{exc} = 325 nm. The luminescence signal resulting from the sensitization of Eu^{III} by 3,4,3-LI(1,2-HOPO) decreases while the Gd^{III} concentration increases.

the ligand[9] (Table 2), as well as the hydrolysis constants of the competing lanthanide ions[16] (See ESI† Table S1), as fixed parameters in the refinements, with the emission intensity resulting exclusively from the sensitization of Eu^{III}, Sm^{III}, or Tb^{III} by 3,4,3-LI(1,2-HOPO). The refined complex formation constants and corresponding pM values are reported in Table 1.

Stability increase along the lanthanide series

The stability of the $[Ln^{III}(3,4,3\text{-LI}(1,2\text{-HOPO}))]^-$ complexes increases along the lanthanide series (Table 1 and Fig. 5), an effect that can be attributed to different reasons: (i) the cation radii size, which decreases along the series,[23,24] (ii) the coordination number of the lanthanide, which can vary from 9 to 8, and thus the number of water molecules in the complex inner sphere,[25,26] and (iii) the Lewis acidity of the metal, which increases along the series.[27]

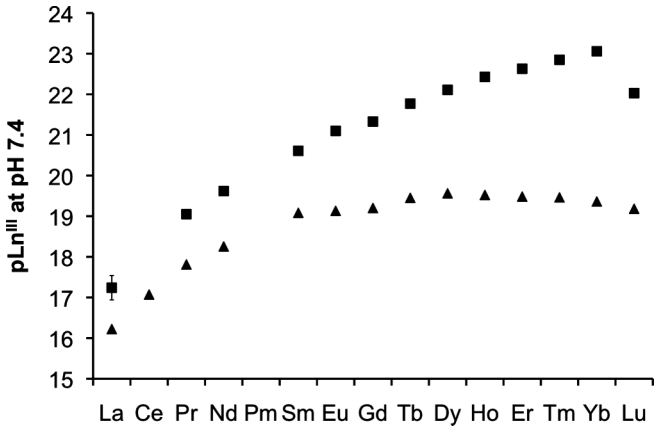

Fig. 5 Comparison of the pM values obtained for the Ln^{III} complexes of 3,4,3-LI(1,2-HOPO) (■) and DTPA[16](▲).

The number of inner sphere water molecules in the Eu^{III} complex was determined previously as zero,[9] using the luminescence-based Horrocks equation,[28] which could not be reliably applied to the other lanthanides. Mass spectrometry was used to characterize the complexes and determine the corresponding coordination number. However, only 8-coordinated complexes could be confirmed in negative ion mode (Fig. 6 and ESI† Table S2).

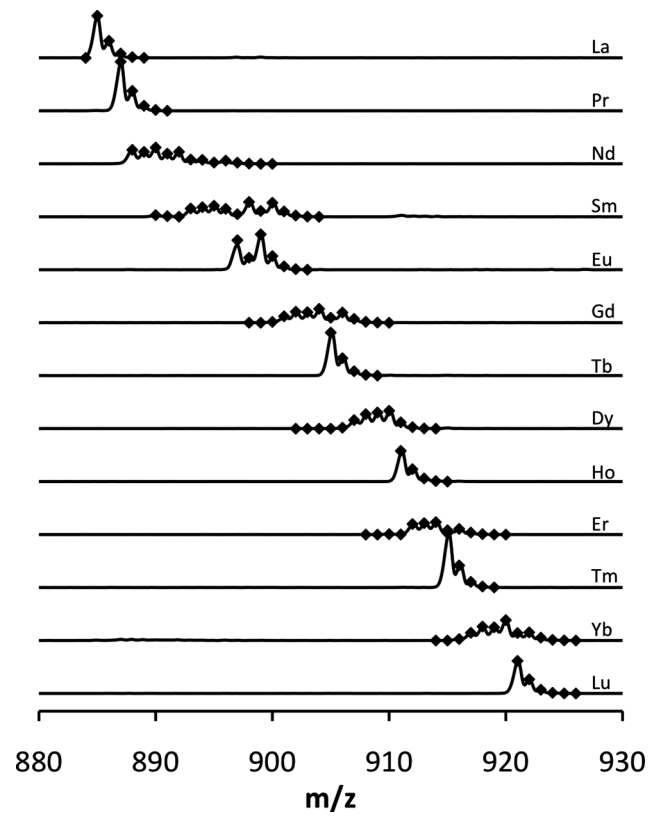

Fig. 6 Mass spectra of 50 μM $[Ln^{III}(3,4,3\text{LI-}(1,2\text{-HOPO}))]^-$ solutions directly injected in the ESI-MS at pH = 7.4 (solid lines). The diamonds represent the theoretical calculated isotope patterns for the complexes.

If an additional water molecule was bound to the metal center, it might be too labile and released during the spraying process. Other techniques such as NMR or X-ray absorption spectroscopies may

be used in the future to characterize and compare the coordination spheres of these metal complexes.

The *in vivo* distribution patterns and biokinetics of the lanthanides have been investigated previously,[29,30] revealing an increase in bone retention and a decrease in liver deposition along the lanthanide series. These patterns may be linked to an increase in lanthanide complex stability with the phosphate binding moieties of the bone matrices, similar to the stability increases observed with 3,4,3-LI(1,2-HOPO), as the metal ion becomes smaller and more acidic. The use of pM values also allows for comparisons between different ligands: the affinity of 3,4,3-LI(1,2-HOPO) for lanthanide cations is remarkably high and at least 1.5 orders of magnitude higher than that of DTPA[16] (Fig. 5). In addition, citrate is a low molecular weight biological ligand that may play a predominant role in lanthanide *in vivo* speciation.[31] However, the stabilities of citrate-lanthanide complexes (pM ranging from 8.3 for La^{III} to 9.0 for Yb^{III})[16] are substantially lower than those determined with 3,4,3-LI(1,2-HOPO). The octadentate hydroxypyridonate chelator can therefore form some of the strongest complexes so far identified with the trivalent metal ions of the lanthanide series, which makes it an excellent candidate for decorporation applications.

In vivo decorporation and stability

To evaluate the efficacy of 3,4,3-LI(1,2-HOPO) at forming stable *in vivo* Eu^{III} complexes and at promoting Eu decorporation, the designed experimental protocols used a ^{152}Eu radiolabel, as well as $CaNa_3$DTPA-treated and untreated control groups. In the decorporation experiment, $^{152}Eu^{III}$ was administered intravenously as a chloride solution (0.008 M sodium citrate, 0.14 M NaCl, pH 4), and the ligands were injected intraperitoneally 1 h later. In the *in vivo* stability experiment, ^{152}Eu-ligand complexes were formed *in situ* (Ligand:Eu ratio > 20) and administered intravenously. Mice were euthanized 24 h after the metal injection, and blood, tissues, and excreta were radioanalyzed for ^{152}Eu content (See ESI† Tables S3 and S4).

When 3,4,3-LI(1,2-HOPO) was administered as a chelating agent, the 24-hour ^{152}Eu body content was significantly reduced to 18% of the injected dose, in comparison to 54 and 67% for $CaNa_3$DTPA-treated and untreated control groups, respectively (Fig. 7). The ^{152}Eu content in the liver and skeleton of mice treated with the experimental ligand was also considerably lower than that in mice treated with $CaNa_3$DTPA. In contrary to $CaNa_3$DTPA, 3,4,3-LI(1,2-HOPO) promoted ^{152}Eu decorporation through a predominant fecal excretion pathway (~64% of the total excretion). These different excretion patterns were also observed in the complex stability experiment: more than 99% of the injected complexes were excreted after 24 h in both cases, however for the DTPA complex ^{152}Eu was mostly found in the urine while nearly 90% of the ^{152}Eu for the-3,4,3-LI(1,2-HOPO) complex was detected in the feces (Fig. 7). The ^{152}Eu decorporation process must therefore follow two different biochemical pathways for both ligands, probably due to the respective membrane permeability properties of the ligands. Overall, these results corroborate the thermodynamic stability constants corresponding to the Eu^{III} complexes of DTPA and 3,4,3-LI(1,2-HOPO): while both ligands form highly stable complexes *in vivo*, the hydroxypyridonate ligand 3,4,3-LI(1,2-HOPO) has a higher affinity for Eu^{III} that enhances its capability to compete with biological ligands such as proteins and bone matrices and thereby its decorporation properties, as compared to DTPA.

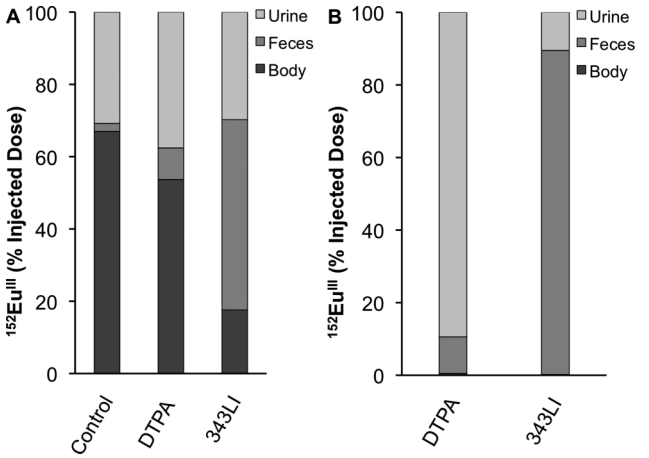

Fig. 7 **A)** Decorporation of ^{152}Eu promoted by injected ligands. Normal mice injected intravenously with ^{152}Eu; ligands (30 μmol kg^{-1}) injected intraperitoneally 1 h later; mice euthanized at 24 h. **B)** *In vivo* stability of ^{152}Eu complexes of DTPA and 3,4,3-LI(1,2-HOPO). Normal mice injected intravenously with ^{152}Eu-ligand complexes; mice euthanized at 24 h.

Conclusions

The stability constants of the lanthanide complexes formed with the hydroxypyridonate ligand 3,4,3-LI(1,2-HOPO) were determined through a new indirect spectrofluorimetric titration method using the remarkable lanthanide luminescence sensitization properties of this chelator. The high affinity of this chelator for lanthanides, as compared to DTPA, indicates its potential as a therapeutic chelating agent for f-block metal ions, which was confirmed through the first *in vivo* decorporation and stability experiments using the radiotracer ^{152}Eu, a common fission product in the nuclear fuel process. Other radionuclides potentially targeted by 3,4,3-LI(1,2-HOPO) include tri- and tetravalent actinides such as Pu^{IV} and Am^{III}. The analytical methods used here will be applied to the determination of the photophysical properties and thermodynamic parameters of the corresponding 3,4,3-LI(1,2-HOPO) complexes, providing a rationale to the use and design of new decorporation agents. In addition, sensing f-block metal ions through luminescence spectroscopy has the potential to ease and significantly improve current actinide detection and characterization methods in terms of selectivity and accuracy.

Acknowledgements

This research was supported by the National Institutes of Health (Lanthanide and Actinide Decorporation Program, Grants AI074065-01, 1RC2AI087604-01 and 5RC2AI087604-02), the Director, Office of Science, Office of Basic Energy Sciences, the Division of Chemical Sciences, Geosciences and Biosciences of the U.S. Department of Energy at LBNL under Contract No. De-AC02-05CH11231 (Lanthanide and Actinide Luminescence Studies).

References

1 P. W. Durbin, *Health Phys.*, 2008, **95**, 465–492.
2 E. G. Moore, C. J. Jocher, J. Xu, E. J. Werner and K. N. Raymond, *Inorg. Chem.*, 2007, **46**, 5468–5470.
3 E. G. Moore, A. P. S. Samuel and K. N. Raymond, *Acc. Chem. Res.*, 2009, **42**, 542–552.
4 R. C. Scarrow, P. E. Riley, K. Abu-Dari, D. L. White and K. N. Raymond, *Inorg. Chem.*, 1985, **24**, 954–967.
5 E. J. Werner, A. Datta, C. J. Jocher and K. N. Raymond, *Angew. Chem., Int. Ed.*, 2008, **47**, 8568–8580.
6 R. J. Abergel, P. W. Durbin, B. Kullgren, S. N. Ebbe, J. Xu, P. Y. Chang, D. I. Bunin, E. A. Blakely, K. A. Bjornstad, C. J. Rosen, D. K. Shuh and K. N. Raymond, *Health Phys.*, 2010, **99**, 401–407.
7 P. W. Durbin, B. Kullgren, S. N. Ebbe, J. Xu and K. N. Raymond, *Health Phys.*, 2000, **78**, 511.
8 R. J. Abergel and K. N. Raymond, *Hemoglobin*, 2011, **35**, 276–290.
9 R. J. Abergel, A. D'Aleo, C. Ng Pak Leung, D. K. Shuh and K. N. Raymond, *Inorg. Chem.*, 2009, **48**, 10868–10870.
10 P. Gans and B. O'Sullivan, *Talanta*, 2000, **51**, 33–37.
11 P. Gans, A. Sabatini, and A. Vacca, *pHab20003*, Leeds, U.K. Florence, Italy.
12 P. Gans, A. Sabatini, and A. Vacca, *HYPERQUAD2000*, Leeds, U.K. Florence, Italy.
13 P. Gans, A. Sabatini and A. Vacca, *Talanta*, 1996, **43**, 1739–1753.
14 P. Gans, A. Sabatini and A. Vacca, *Ann. Chim.*, 1999, **89**, 45–49.
15 P. Gans, A. Sabatini, and A. Vacca, *HypSpec*, Leeds, U.K. Florence, Italy.
16 A. E. Martell, R. M. Smith, and R. J. Motekaitis, *NIST Standard Reference Database 46*.
17 L. Alderighi, P. Gans, A. Ienco, D. Peters, A. Sabatini and A. Vacca, *Coord. Chem. Rev.*, 1999, **184**, 311–318.
18 L. Alderighi, P. Gans, A. Ienco, D. Peters, A. Sabatini, and A. Vacca, *HYSS*, Leeds, U.K. Florence, Italy.
19 P. W. Durbin, N. Jeung, B. Kullgren and G. K. Clemons, *Health Phys.*, 1992, **63**, 427–442.
20 P. W. Durbin, B. Kullgren, J. Xu and K. N. Raymond, *Radiat. Protect. Dosim.*, 1994, **53**, 305–309.
21 P. W. Durbin, B. Kullgren, J. Xu, K. N. Raymond, P. G. Allen, J. J. Bucher, N. M. Edelstein and D. K. Shuh, *Health Phys.*, 1998, **75**, 34–50.
22 J.-C. G. Bünzli and C. Piguet, *Chem. Soc. Rev.*, 2005, **34**, 1048.
23 M. Seitz, A. G. Oliver and K. N. Raymond, *J. Am. Chem. Soc.*, 2007, **129**, 11153–11160.
24 R. D. Shannon, *Acta Crystallogr., Sect. A: Cryst. Phys., Diffr., Theor. Gen. Crystallogr.*, 1976, **32**, 751–767.
25 K. Djanashvili and J. A. Peters, *Contrast Media Mol. Imaging*, 2007, **2**, 67–71.
26 K. Djanashvili, C. Platas-Iglesias and J. A. Peters, *Dalton Trans.*, 2008, 602.
27 H. Tsuruta, K. Yamaguchi and T. Imamoto, *Tetrahedron*, 2003, **59**, 10419–10438.
28 R. M. Supkowski and W. D. Horrocks, *Inorg. Chim. Acta*, 2002, **340**, 44–48.
29 P. W. Durbin, *Health Phys.*, 1960, **2**, 225.
30 D. M. Taylor and R. W. Leggett, *Radiat. Protect. Dosim.*, 2003, **105**, 193–198.
31 A. Heller, A. Barkleit and G. Bernhard, *Chem. Res. Toxicol.*, 2011, **24**, 193–203.

